

CheMFi: A Multifidelity Dataset of Quantum Chemical Properties of Diverse Molecules

Vivin Vinod* and Peter Zaspel*

School of Mathematics and Natural Science, University of Wuppertal, 42119 Wuppertal, Germany

E-mail: vinod@uni-wuppertal.de; zaspel@uni-wuppertal.de

Abstract

Progress in both Machine Learning (ML) and conventional Quantum Chemistry (QC) computational methods have resulted in high accuracy ML models for QC properties ranging from atomization energies to excitation energies. Various datasets such as MD17, MD22, and WS22, which consist of properties calculated at some level of QC method, or fidelity, have been generated to benchmark such ML models. The term fidelity refers to the accuracy of the chosen QC method to the actual real value of the property. The higher the fidelity, the more accurate the calculated property, albeit at a higher computational cost.

Research in multifidelity ML (MFML) methods, where ML models are trained on data from more than one numerical QC method, has shown the effectiveness of such models over single fidelity methods. Much research is progressing in this direction for diverse applications ranging from energy band gaps to excitation energies. A major hurdle for effective research in this field of research in the community is the lack of a diverse multifidelity dataset for benchmarking.

Here, we present a comprehensive multifidelity dataset drawn from the WS22 molecular conformations. We provide the quantum Chemistry MultiFidelity (CheMFi) dataset

consisting of five fidelities calculated with the TD-DFT formalism. The fidelities differ in their basis set choice and are namely: STO-3G, 3-21G, 6-31G, def2-SVP, and def2-TZVP. ChemFi offers to the community a variety of QC properties including vertical excitation energies, oscillator strengths, molecular dipole moments, and ground state energies. In addition to the dataset, multifidelity benchmarks are set with state-of-the-art MFML and optimized-MFML.

Keywords: machine learning, multifidelity machine learning, dataset, Wigner sampling, quantum chemistry, DFT, orca software

1 Background and Summary

Recent developments in the field of machine learning (ML) for quantum chemistry (QC) have significantly changed the landscape of research and discovery in QC properties¹⁻⁴. This has allowed significant reduction in the time to calculate (or rather, predict) QC properties once an ML model has been trained. For such models, the protocol involves testing them against some benchmark datasets such as the MD17⁵, QM7⁶, or the QM9 dataset^{7,8}. The MD17 dataset consists of trajectories of small to medium-sized molecules with their corresponding geometries, forces, and potential energies. In contrast, the QM7 and QM9 datasets are collections of various molecules and their isomers with properties ranging from dipole moments to enthalpies. These diverse datasets allow for a uniform assessment of ML methods for QC. Recently, the WS22 database was released with a collection of Wigner Sampled geometries of 10 diverse molecules^{9,10}. With varied chemical complexity and number of atoms, the WS22 datasets provides a collection of QC properties for these molecules calculated at one level of theory, or *fidelity*. It was also shown that for this collection of molecules the use of ML methods is indeed challenging. This is primarily due to the wider chemical space that the Wigner Sampled geometries cover^{9,11}.

The usual method of training a ML model on a required level of QC theory has since been superseded by methodological improvements which harness inherent QC hierarchies to cancel out errors in different numerical QC methods. These are categorized as multifidelity methods. The most elementary multifidelity method, called Δ -ML, involves the use of two QC methods, or fidelities, one significantly cheaper than the other¹². An ML model is trained on the difference between these two fidelities. Recently, a systematic generalization of the Δ -ML method was implemented for excitation energies and termed multifidelity machine learning (MFML)¹³ where more than two fidelities are used to train various ML models resulting in low-cost high-accuracy MFML model. Yet another multifidelity method which has been shown to be efficient in potential energy surface (PES) reconstruction is the hierarchical-ML (h-ML) approach¹⁴. In h-ML, an *ad hoc* optimization is carried out to select the ideal number of training samples across various fidelities to build one composite multifidelity model. The optimized MFML method was introduced in Ref.¹⁵ where the combination of the different sub-models built on different fidelities is optimized on a holdout validation set of reference properties. Such an o-MFML was shown to improve the accuracy of prediction for atomization energies and excitation energies across diverse molecules. Certain other flavors of ML using multifidelity data have been proposed and tested, including multi-task Gaussian processes treating the different fidelities as interdependent tasks^{16,17}. Also, various multifidelity methods have been applied to predicting diverse QC properties such as band gaps in solids, excitation energies, and atomization energies of various molecules^{13,18-20}.

With significant push in the direction of research and development in the multifidelity methods, it becomes important to also follow protocols similar to the single fidelity ML methods. That is, there is a need for uniform benchmarking of multifidelity models for their accuracy of prediction, ease of transferability of the models, and reducing cost of generating training data among other things. Therefore, a diverse set of multifidelity data is needed to uniformly assess the various developed and developing multifidelity models in the area of ML for QC. One such dataset that exists is the QM7b^{6,21} which is an extension

of the QM7 dataset. Originally created for multi-task learning, it has since been used in the methodological benchmarking of multifidelity models with atomization energies being calculated at three levels of theory with three varying basis set sizes^{15,20}. Although the highest level of theory used in this dataset is the gold standard Coupled Cluster Singles and Doubles perturbative Triples (CCSD(T)), it provides a limited possibility to assess the effectiveness of multifidelity methods due to its small size, 7,211 samples. This is indeed a small amount of data to enable proper benchmarking of multifidelity methods. In addition to this, the QM7b is a collection of only small to medium sized molecule with the number of atoms ranging from 4 to 23. Further, as recent studies have shown, multifidelity methods tend to behave differently for different properties ranging from atomization energies to excitation energies to band gaps in polymers^{15,19,20}. This results in independent and uncorrelated developments of the multifidelity method which although displaying benefit for one property might fall short, while being used for another QC property.

To unify the research in this rapidly developing field of multifidelity methods, it becomes necessary to present to the community a diverse collection of multifidelity data over a range of molecular complexity. Building up on existing datasets is preferred in such a scenario to prevent redundant calculations and geometry generation. After all, the entire point of a multifidelity method is to reduce compute cost and resource usage in discovery and research. In interest of such an approach, the WS22 database¹⁰ was chosen to be the collection of geometries. In addition to being a collection of molecules that are chemically complex with distinct conformers, the molecule in this dataset also cover a wide range of the quantum chemical configuration space in contrast to other datasets such as MD17. The presence of flexible functional groups make the geometries, and by extension, the QC properties, of this dataset challenging for ML models to learn. These features make this collection the preferred choice to generate multifidelity data. For each of the molecules of increasing size and chemical complexity, this dataset offers 120,000 geometries. This creates a vast dataset collection of diverse geometries covering various conformers of the different molecules. In total there are

around 1 million geometries in the WS22 database. Performing multifidelity QC calculations for such a vast number of geometries is not feasible. It is more realistic and computationally feasible to produce a multifidelity dataset for a portion of the geometries of the WS22 database. Therefore, for each of the molecules in the WS22 database, 15,000 geometries were evenly sampled (see supplementary material section S1 for more details) and the multifidelity QC calculations performed for these. Thus, in total, $9 \times 15,000 = 135,000$ geometries were sampled and the multifidelity data was computed for these. This dataset is provided to the ML-QC community under the name CheMFi (quantum **C**hemistry **M**ulti**F**idelity) dataset²². A detailed description of the geometry sampling, data generation procedure, the fidelities, and the technical details of the CheMFi dataset are provided in the following section. In addition, scripts to generate two multifidelity models from Ref. ¹⁵ are provided. These are multifidelity machine learning (MFML) and optimized MFML (o-MFML) models. The ML methods such as MFML and o-MFML are discussed in the supplementary materials in Section S2 to retain readability of this main text.

The diverse collection of molecules in CheMFi along with their multifidelity properties, provides a challenging dataset for the domain of ML in QC. Due to the large number of multifidelity data points, and easily usable associated scripts, we believe that CheMFi is a significant collection that will help push the boundaries of multifidelity methods for ML in QC properties.

2 Methods

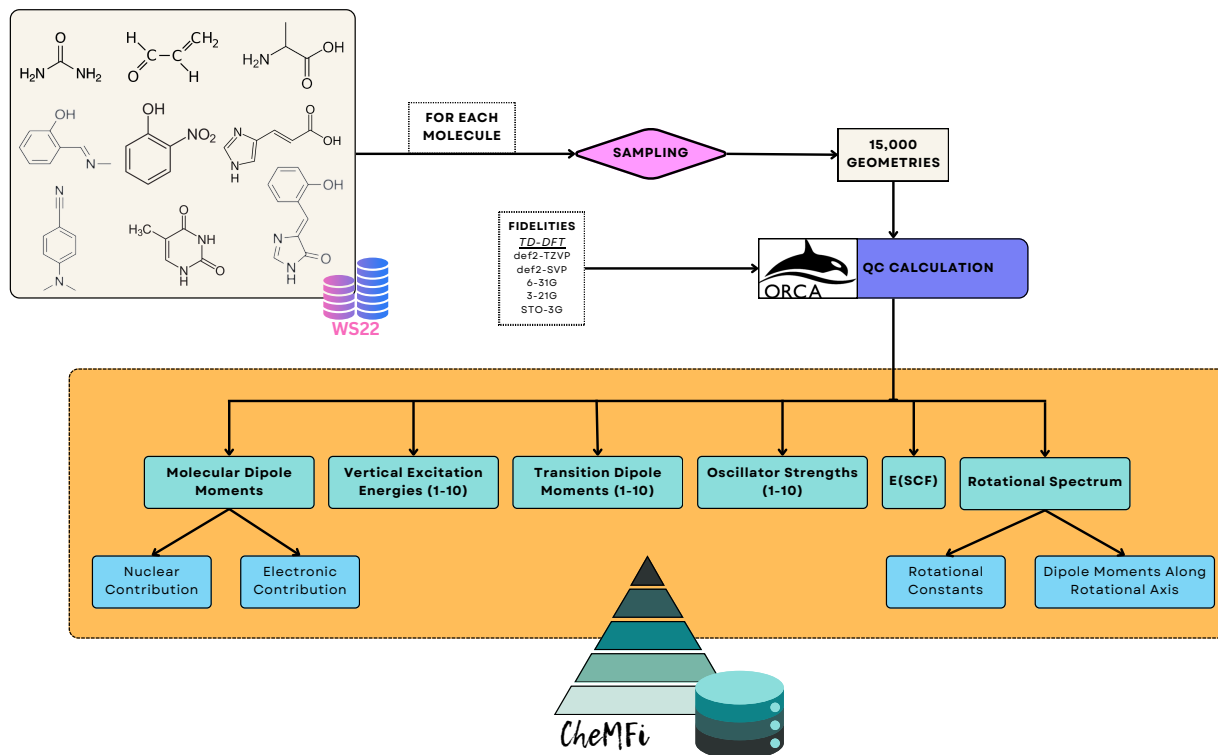


Figure 1: The workflow of generating the CheMFi dataset by sampling from the WS22 database. 15,000 geometries are used for each molecule resulting in a total of 135,000 single point geometries. For each of these, multiple QC properties are calculated at DFT level of theory with varying basis set sizes to create the diverse multifidelity dataset. Molecular geometry images taken from Wikimedia Commons and Ref.⁹.

The original WS22 database includes the following molecules (in increasing order of number of atoms):

1. urea
2. acrolein
3. alanine
4. 2-(methyliminomethyl)phenol (SMA)
5. 2-nitrophenol

6. urocanic acid
7. 4-(dimethylamino)benzotrile (DMABN)
8. thymine
9. 4-(2-hydroxybenzylidene)-1,2-dimethyl-1H-imidazol-5(4H)-one (o-HBDI)

In addition to these molecules, toluene is also included to compare with the MD17⁵ database. Since toluene consists of a single conformer and was only introduced in WS22 for comparison to existing datasets such as MD17, this molecule was not included while generating the CheMFi dataset. The original WS22 database was first generated as reported extensively in Ref.⁹. The pipeline involves optimized equilibrium geometries identification for the different conformations of the molecule with DFT^{23,24}. Following this, the respective Wigner Sampling is carried out from ground state (S0) and/or excited state (S1) minima. For these, the geometries are subsequently interpolated by finding on a Riemann manifold, an optimized geodesic curve. The metric for this is defined by a redundant internal coordinate functions²⁵. In the original WS22 database provided in Ref.¹⁰, this results in a little over 1 million samples across 9 molecules with various properties calculated at the TD-DFT level of theory using the PBE0/6-311 G* functional and basis set combination⁹.

To build the CheMFi dataset from the WS22 database, 15,000 geometries were sampled from the original 120,000 geometries for each of these molecules. These were evenly sampled across the 120,000 geometries to ensure even coverage of the chemical space. Further details of the sampling are mentioned in the supplementary material Section S1. An even sampling of the original dataset ensures that there are sufficient geometries from all conformations of the molecule. In order to verify that this form of sampling did in fact cover even chemical space, UMAPs²⁶ were studied and the results were satisfactory indicating the uniform coverage of the chemical space. These UMAPs and related discussion on the inferences are reported in the supplementary section S1. Once these geometries were sampled, they were used to

perform point calculations for the QC properties. The complete workflow of the dataset generation process is pictorially depicted in Figure 1.

Table 1: List of properties available in the CheMFi dataset. The corresponding dimension(s) and units of the properties are also given with the npz file key. †From the WS22 database^{9,10}

PROPERTY	DIMENSIONS/UNITS	npz ID
Atomic Numbers [†]	(n_atoms,)	‘Z’
Cartesian Coordinates [†]	(n_atoms,)/Å	‘R’
E(SCF)	(15000, 5)/hE	‘SCF’
Vertical Excitation Energies	(15000, 5, 10)/cm ⁻¹	‘EV’
Transition Dipole Moments	(15000, 5, 10, 3)/a.u.	‘TrD’
Oscillator Strength	(15000, 5, 10)	‘fosc’
Molecular Dipole Moment (electronic)	(15000, 5, 3)/a.u.	‘DPe’
Molecular Dipole Moment (nuclear)	(15000, 5, 3)/a.u.	‘DPn’
Rotational Constants	(15000, 5, 3)/cm ⁻¹	‘RCo’
Dipole Moment Along Rotational Axis	(15000, 5, 3)/a.u.	‘DPRo’

For the 9 molecules taken from the WS22 database, after 15,000 geometries were evenly sampled, QC calculations were performed at the TD-DFT level of theory with the CAM-B3LYP functional. For each geometry, five fidelities were calculated. These fidelities are the basis set choice of increasing size. In increasing hierarchy of the fidelity, these are: STO-3G, 3-21G, 6-31G, def2-SVP, and def2-TZVP. In the rest of the document, for the most part, these are referred to by their short-hand, i.e., STO3G up to TZVP. The `TightSCF` keyword was employed to ensure energy convergence of the order of 10^{-9} a.u. for each calculation. Resolution of Identity approximation (RIJCOSX) was employed in order to speed up the excitation energy calculations. For any calculation, the maximum memory usage was limited to 2.0 GB. In practice, the ORCA calculations did not use this amount of memory. A total of 10 vertical excitation energies were calculated with each fidelity for each geometry.

A note on the calculations being restricted to DFT methods is to be made here. Since CheMFi is a benchmark dataset and not a high accuracy model training dataset, the cost of generating a costlier dataset, say at coupled cluster level of theory, was considered to be excessive. The aim of this dataset is to present a diverse collection of QC properties based on a set of complex molecules which can be used to uniformly assess MFML methods.

Therefore, the QC properties are calculated only with DFT methods and higher accuracy methods such as the gold standard CCSD(T) are not considered.

All calculations were performed with the ORCA(5.0.1) quantum chemistry package²⁷. From these calculations, a diverse set of QC properties were extracted including information of the vertical excitation states such as energies and oscillator strengths. The list of available multifidelity properties is given in Table 1. The Cartesian coordinates and atomic numbers are taken from the WS22 database. The SCF energies are reported in Hartree units. The first 10 vertical excitation energies are provided in cm^{-1} with their corresponding oscillator strengths and transition dipole moments (in a.u.). The molecular dipole moments are also a property included in the CheMFi dataset with both the nuclear and electronic contributions being separately cataloged in atomic units (a.u.). The rotational spectrum data is also included in the form of Rotational Constants (in cm^{-1}) and the total molecular dipole moments (in a.u.) aligned along rotational axes. Details of data hosting and storage are reported in Section 3.

This diverse collection of QC properties is made available for $9 \times 15,000 = 135,000$ geometries across five different fidelities making CheMFi the most elaborate multifidelity database generated at the time of submission/publication. This collection of multifidelity QC properties provides ample room for development and benchmarking of MFML methods and models.

3 Data Records

The various QC properties of the CheMFi dataset are stored in separate NumPy (v 1.26.4) `npz` files for each molecule. These `npz` files have a dictionary-like format allowing for each property to be accessed via its corresponding key denoted in Table 1. Each property itself is stored as a NumPy `ndarray` with the first dimension being 15,000 corresponding to the number of geometries. Thus, the QC properties can be accessed by querying the right ID.

```
import numpy as np
#load the dataset for alanine
data = np.load('CheMFi_alanine.npz')
#query for the vertical excitation energies
EV = data['EV']
#Select the second vertical state for SVP (4th fidelity)
EV_SVP = EV[:,3,1]
#note that Python arrays start with 0
```

Listing 1: Python example to extract the SVP fidelity values of second vertical excitation state of alanine from ChemFi.

For example, the SCF energies can be accessed with the key 'SCF' returning a NumPy ndarray of size $15,000 \times 5$ where the second dimension of the array corresponds to the five fidelities used. An example script to accessing the QC properties is shown in Listing 1.

The dataset itself is hosted on Zenodo at <https://zenodo.org/records/11636903> with a detailed README file documenting the key aspects of the dataset²². The README also provides information on how to access the different properties using Python. For the ChemFi dataset, the various scripts involved in generating the data, including ORCA input files and shell scripts to extract properties from the ORCA log files, are stored in the code repository that can be accessed at <https://github.com/SM4DA/CheMFi>. In addition to these scripts, the code repository also contains Python scripts to perform multifidelity benchmarks on this dataset. These can be launched using the CLI and are a handy tool in setting benchmarks for this dataset using current state of art multifidelity methods.

4 Technical Validation

To validate the ChemFi dataset, The MFML and o-MFML models prescribed in Ref.¹⁵ were tested in predicting SCF energies and the first vertical excitation energies. The multifidelity models are built for different baseline fidelities, which refers to the cheapest fidelity included in the model. For example, a baseline fidelity $f_b = 631\text{G}$ implies that the multifidelity model is built up of the fidelities 631G, SVP, and TZVP¹⁵.

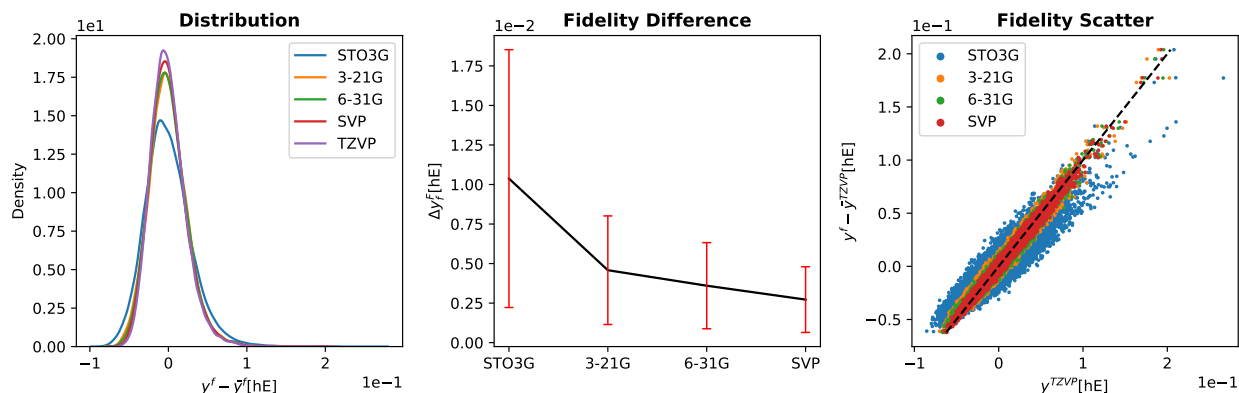
In addition to benchmarking the multifidelity models on properties of individual molecules, the models are also tested on using all the molecules of the dataset. For this purpose, the SCF property of all molecules are used to train one single MFML and o-MFML model. This is then tested on predicting the SCF energies of all molecules.

While these two broad tests serve as a benchmark for multifidelity models on this dataset, the benchmarks of the other properties and molecules are not reported here. However, it is to be pointed out that the scripts provided can be readily used to generate benchmarks for these cases using standard ML methods such as learning curves. All learning curves are reported for a 10-run average, that is, for 10 random shuffling of the training set as directed in Ref. [15](#).

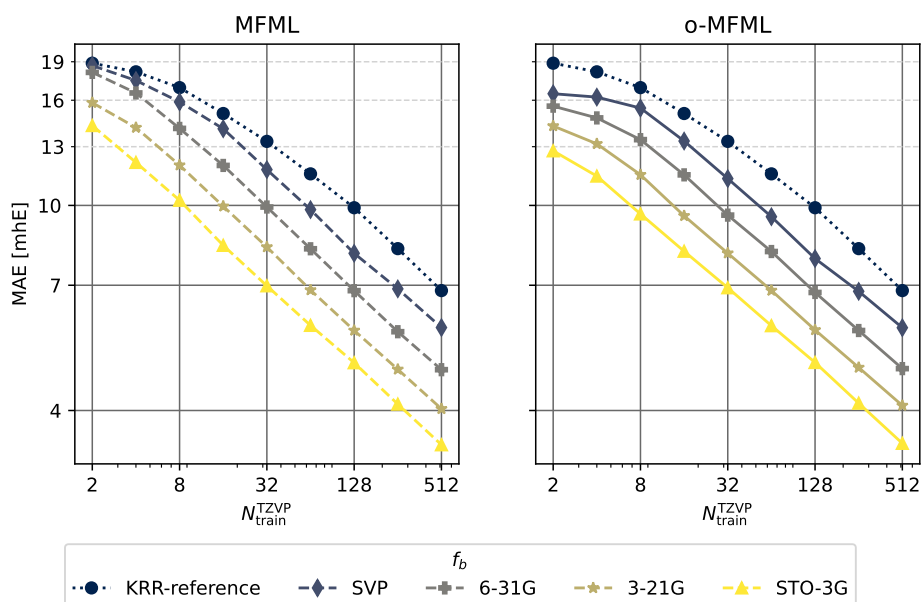
4.1 Single Molecule Benchmarks

The technical validation carried out individually for SMA and o-HBDI molecules is in line with the experimental set-up of Ref. [13](#). A total of 12,288 training samples were chosen to build the multifidelity models. 712 samples were set aside as a validation set for the o-MFML model from Ref. [15](#), and the remaining 2,000 samples were used as a test set. The accuracy of the models are gauged with mean absolute error (MAE) in the form of learning curves. Learning curves display the MAE with respect to increasing number of training samples, here, at the highest fidelity, that is, TZVP.

Figure [2](#) reports the multifidelity benchmarking process for SCF energies for SMA. The SLATM molecular descriptor^{[28](#)} was used with a Laplacian kernel to perform kernel ridge regression (more details in Supplementary Information Section S2). First, the preliminary analyses as recommended by Ref. [13](#) are shown in Figure [2a](#). These are recommended preliminary investigation of multifidelity data. The first of these is to study the distribution of the multifidelity data. The second analysis is the study of mean absolute differences between each fidelity and the target fidelity (that is, the most accurate fidelity, here, TZVP). Generally, it is anticipated that these differences decay monotonically for increasing fidelity. Thirdly and



(a) Preliminary analysis of multifidelity structure of SCF energies for the SMA molecule. The three different preliminary tests for the hierarchy are performed as prescribed in Ref. [13](#).



(b) Learning curves for MFML and o-MFML for the SCF property of SMA as recorded in the ChemFi database. The reference single-fidelity KRR is also shown by training on TZVP only. The Laplacian kernel was used with a kernel width of 200.0 and regularization of 10^{-10} . The Global SLATM²⁸ molecular descriptors were used.

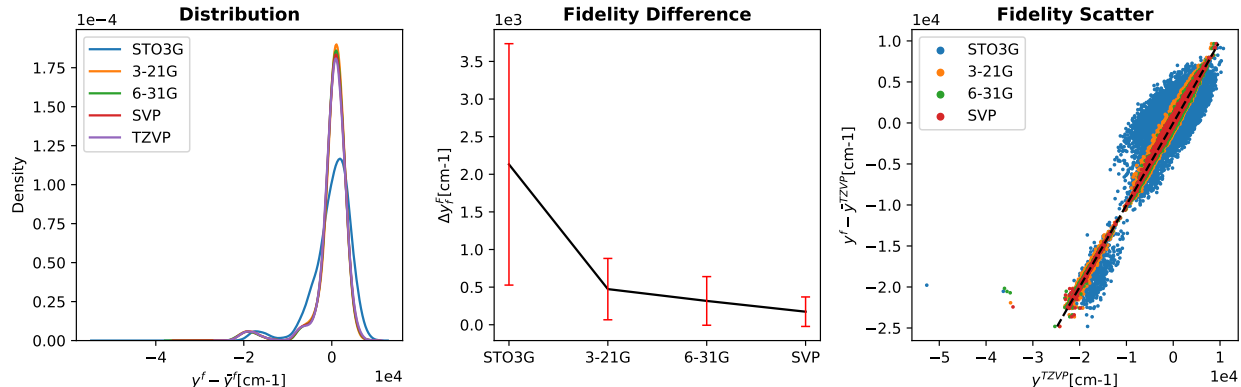
Figure 2: Technical benchmarks of SMA from the ChemFi dataset.

finally, the scatter of the fidelities with respect to the target fidelity is generated to study how these deviate with respect to the target fidelity. The three different preliminary analyses show a systematic ordering of the fidelities giving a nod to the assumed hierarchy as seen in the fidelity difference plots. The fidelity scatter plot also shows a systematic distribution of the energies when compared to the target fidelity of TZVP. In Ref. [13](#) this was identified

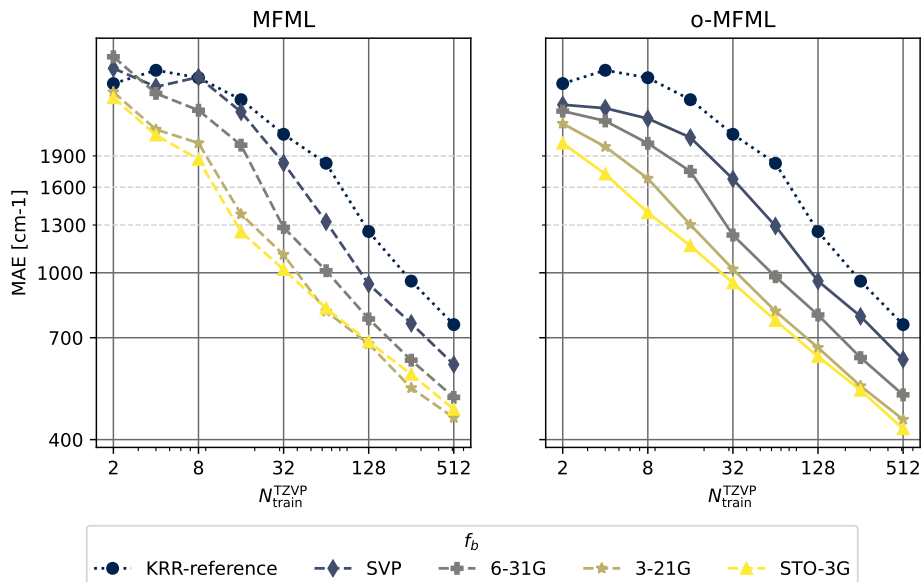
as a good preliminary indicator of favorable results in the MFML models. In Figure 2b, the learning curves of MFML and o-MFML (with OLS optimization) are depicted for the prediction of SCF energies. The multifidelity learning curves can be understood as follows: the addition of a cheaper fidelity systematically decreases the error (here reported as mean absolute error, MAE) which is reported in units of milli-Hartree. With each cheaper fidelity being added, one notices that the corresponding learning curve from Figure 2b has a lower offset. The continuing negative slope indicates that further addition of training samples could decrease the MAE of these models. There is no significant difference in MAE between the MFML and o-MFML models and they both perform similarly for the prediction of SCF.

A similar benchmarking procedure was carried out for the prediction of first vertical excitation energies of o-HBDI. In this case, the unsorted CM were used with the Matérn Kernel. Further details are presented in Section S2 of the supplementary file. As for the case of SMA, a preliminary analysis study was performed with the resulting plots shown in Figure 3a. The difference in fidelities plot in the center indicates that the assumed hierarchy holds true for the fidelities. However, the fidelity scatter plot on the right hand side shows two distinct clusters. These correspond to the two main conformers of o-HBDI, namely the cis and trans conformers. The scatter also shows some cases where the STO3G fidelity covers a wider range of values and is less localized than the other fidelities. This could indicate that the use of STO3G in the MFML models would result in a lower improvement of the accuracy of the model.

The learning curves for the prediction of the first vertical excitation energies of o-HBDI from ChemFi are shown in Figure 3b. The MAE are reported in cm^{-1} with the axes identically scaled for both MFML and o-MFML. With the addition of cheaper fidelities, the learning curves show a constant reduction in the offset of the MAE as seen in the near parallel learning curves of the different baseline fidelities. As anticipated from the preliminary analysis, the addition of the STO3G fidelity does not provide significant improvement especially for larger training samples. However, this is rectified, as expected, by the o-MFML



(a) Preliminary analysis of multifidelity structure of the first vertical excitation energies for the o-HBDI molecule. The three different preliminary tests for the hierarchy are performed as prescribed in Ref. ¹³.



(b) Learning curves for MFML and o-MFML for the first vertical excitation energy of o-HBDI from the ChemFi database. The reference single-fidelity KRR is also shown by training on TZVP only. The Matérn kernel of first order with L_2 -norm was used with a kernel width of 150.0 and regularization of 10^{-10} . Unsorted CM descriptors were used for these cases.

Figure 3: Technical benchmarks of o-HBDI from the ChemFi dataset.

method which was indeed shown to fix this very issue in Ref. ¹⁵.

4.2 Cumulative use of the dataset

The ChemFi dataset contains multifidelity QC properties of 9 molecules for 15,000 geometries. This totals to $9 \times 15,000 = 135,000$ point calculations of the QC properties. This is

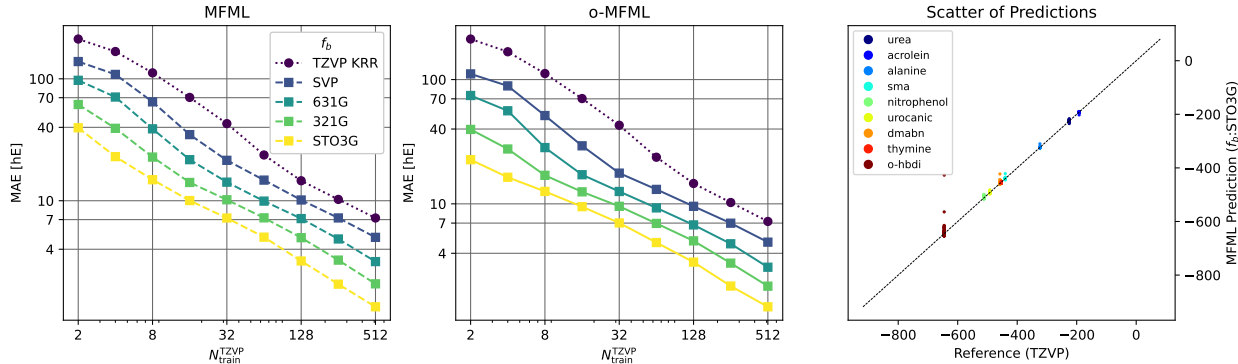


Figure 4: Learning curves for MFML and o-MFML for SCF energies based on the compounded use of the ChemFi dataset. 1,500 samples were randomly chosen from each molecule to perform this example test.

therefore the largest collection of multifidelity dataset which can be used in various benchmarking processes. To demonstrate this form of cumulative use of the dataset, multifidelity models from Ref. ¹⁵ were tested against this in predicting the SCF of the molecules. From each molecule of the ChemFi dataset, 1,500 geometries were randomly chosen and compiled into a total of $9 \times 1,500 = 13,500$ data points. From the 13,500 samples, a random set of 11,000 samples were used as the multifidelity training data. Of the remaining, 500 samples were used as a validation set and 2,000 as the holdout test set. With this setup learning curves were generated for the different multifidelity models in the same fashion as prescribed in Ref. ¹⁵.

The results of this test are shown in Figure 4 for MFML and o-MFML models. The learning curves show a decreasing slope for both cases for the different baseline fidelities. The addition of each cheaper fidelity results in a lower offset of MAE. The constant slope on the log-log axis indicates that addition of training samples can further decrease the MAE. On the right-hand side plot the scatter of reference TZVP versus MFML predicted SCF values are delineated. Across the energy ranges the MFML model predicts the SCF energies accurately as can be inferred from the scatter of the values being close to the identity mapping line.

```
# this code is running in an activated conda environment
(conda) $ python PrelimAnalysis.py -m='sma' \
-d='../dataset/' \
-p='SCF' \
-u='hE' \
--centeroffset \
--saveplot
```

Listing 2: Python example to perform preliminary analysis of SCF multifidelity data for the SMA molecule.

5 Usage Notes

In addition to the multifidelity dataset, various tools to assess and benchmark multifidelity methods are also provided. These include scripts to perform preliminary analysis of the data based on the property of choice as recommended in Ref.¹³, and the scripts to produce learning curves. Further, scripts to generate unsorted Coulomb Matrices, and the global SLATM descriptors are provided which are built upon the qmlcode package²⁹. The scripts are easy to use and well documented allowing for a streamlined benchmarking process with an example shown in Listing 2 for the preliminary analysis. Listing 3 shows an example to generate the multifidelity learning curves.

Associated Content

Supplementary sections S1-S2, Figure S1.

Data availability

The dataset is hosted as an open sourced and citable repository on Zenodo at the URL <https://zenodo.org/records/11636903>.


```

# this code is running in an activated conda environment
(conda) $ python LearningCurves.py -m='sma' \
-d='../dataset/' \
-p='SCF' \
-n=10 \
-w=200.0 \
-rep='CM' \
-k='laplacian' \
-r=1e-10 \
--seed=42 \
--centeroffset

#this creates the various MAE files in npy format
#the following command will plot the learning curves as a PDF file
(conda) $ python LC_plots.py -m='sma' \
-p='SCF' \
-u='hE' \
-rep='CM' \
--centeroffset \
--saveplot

```

Listing 3: Python example to generate multifidelity learning curves and the corresponding plot of SCF for the SMA molecule.

Code availability

All scripts needed to assess this dataset are hosted at <https://github.com/SM4DA/CheMFi>.

This includes scripts to run ORCA calculations, extract properties from the output log files, generating CM and SLATM molecular descriptors, and generating learning curves.

Acknowledgments

The authors acknowledge support by the DFG through projects ZA 1175/3-1 as well as through the DFG Priority Program SPP 2363 on “Utilization and Development of Machine Learning for Molecular Applications – Molecular Machine Learning”. The computations of the quantum chemical properties were carried out on the [PLEIADES cluster](#) at the University of Wuppertal, which was supported by the Deutsche Forschungsgemeinschaft (DFG, grant No. INST 218/78-1 FUGG) and the Bundesministerium für Bildung und Forschung (BMBF). The authors would also like to thank the ‘Interdisciplinary Center for Machine Learning and

Data Analytics (IZMD)’ at the University of Wuppertal.

Declarations

The authors declare that there is no conflict of interest or any competing interests.

References

- (1) Westermayr, J.; Marquetand, P. Machine Learning for Electronically Excited States of Molecules. *Chem. Rev.* **2020**, *121*, 9873–9926.
- (2) Manzhos, S.; Carrington, T. J. Neural Network Potential Energy Surfaces for Small Molecules and Reactions. *Chem. Rev.* **2021**, *121*, 10187–10217, PMID: 33021368.
- (3) Dral, P. O. Quantum chemistry in the age of machine learning. *J. Phys. Chem. Lett.* **2020**, *11*, 2336–2347.
- (4) Dral, P. O.; Barbatti, M. Molecular Excited States through a Machine Learning Lens. *Nat. Rev. Chem.* **2021**, *5*, 388–405.
- (5) Chmiela, S.; Tkatchenko, A.; Sauceda, H. E.; Poltavsky, I.; Schütt, K. T.; Müller, K.-R. Machine learning of accurate energy-conserving molecular force fields. *Sci. Adv.* **2017**, *3*, e1603015.
- (6) Blum, L. C.; Reymond, J.-L. 970 Million Druglike Small Molecules for Virtual Screening in the Chemical Universe Database GDB-13. *J. Am. Chem. Soc.* **2009**, *131*, 8732–8733, PMID: 19505099.
- (7) Ruddigkeit, L.; van Deursen, R.; Blum, L. C.; Reymond, J.-L. Enumeration of 166 Billion Organic Small Molecules in the Chemical Universe Database GDB-17. *J. Chem. Inf. Model.* **2012**, *52*, 2864–2875.

- (8) Ramakrishnan, R.; Dral, P.; Rupp, M.; von Lilienfeld, O. Quantum chemistry structures and properties of 134 kilo molecules. *Sci. Data* **2014**, *1*, 140022.
- (9) Pinheiro Jr, M.; Zhang, S.; Dral, P. O.; Barbatti, M. WS22 database, Wigner Sampling and geometry interpolation for configurationally diverse molecular datasets. *Sci. Data* **2023**, *10*, 95.
- (10) Jr, M. P.; Zhang, S.; Dral, P. O.; Barbatti, M. WS22 database: combining Wigner Sampling and geometry interpolation towards configurationally diverse molecular datasets. 2022; <https://doi.org/10.5281/zenodo.7032334>.
- (11) Hou, Y.-F.; Ge, F.; Dral, P. O. Explicit Learning of Derivatives with the KREG and pKREG Models on the Example of Accurate Representation of Molecular Potential Energy Surfaces. *J. Chem. Theory Comput.* **2023**, *19*, 2369–2379.
- (12) Ramakrishnan, R.; Dral, P. O.; Rupp, M.; von Lilienfeld, O. A. Big Data Meets Quantum Chemistry Approximations: The Δ -Machine Learning Approach. *J. Chem. Theory Comput.* **2015**, *11*, 2087–2096.
- (13) Vinod, V.; Maity, S.; Zaspel, P.; Kleinekathöfer, U. Multifidelity Machine Learning for Molecular Excitation Energies. *J. Chem. Theory Comput.* **2023**, *19*, 7658–7670, PMID: 37862054.
- (14) Dral, P. O.; Owens, A.; Dral, A.; Csányi, G. Hierarchical machine learning of potential energy surfaces. *J. Chem. Phys.* **2020**, *152*, 204110.
- (15) Vinod, V.; Kleinekathöfer, U.; Zaspel, P. Optimized multifidelity machine learning for quantum chemistry. *Mach. learn.: sci. technol.* **2024**, *5*, 015054.
- (16) Fisher, K.; Herbst, M.; Marzouk, Y. Multitask methods for predicting molecular properties from heterogeneous data. 2024; <https://arxiv.org/abs/2401.17898v2>.

- (17) Ravi, K.; Fediukov, V.; Dietrich, F.; Neckel, T.; Buse, F.; Bergmann, M.; Bungartz, H.-J. Multi-fidelity Gaussian process surrogate modeling for regression problems in physics. 2024; <https://arxiv.org/abs/2404.11965>.
- (18) Pilania, G.; Gubernatis, J. E.; Lookman, T. Multi-fidelity machine learning models for accurate bandgap predictions of solids. *Comput. Mat. Sci.* **2017**, *129*, 156–163.
- (19) Patra, A.; Batra, R.; Chandrasekaran, A.; Kim, C.; Huan, T. D.; Ramprasad, R. A multi-fidelity information-fusion approach to machine learn and predict polymer bandgap. *Comput. Mat. Sci.* **2020**, *172*, 109286.
- (20) Zaspel, P.; Huang, B.; Harbrecht, H.; Von Lilienfeld, O. A. Boosting Quantum Machine Learning Models with a Multilevel Combination Technique: Pople Diagrams Revisited. *J. Chem. Theory Comput.* **2019**, *15*, 1546–1559.
- (21) Montavon, G.; Rupp, M.; Gobre, V.; Vazquez-Mayagoitia, A.; Hansen, K.; Tkatchenko, A.; Müller, K.-R.; von Lilienfeld, O. A. Machine learning of molecular electronic properties in chemical compound space. *New. J. Phys.* **2013**, *15*, 095003.
- (22) Vinod, V.; Zaspel, P. CheMFi: A Multifidelity Dataset of Quantum Chemical Properties of Diverse Molecules. 2024; <https://doi.org/10.5281/zenodo.11636903>.
- (23) Quiñonero, D.; Garau, C.; Frontera, A.; Ballester, P.; Costa, A.; Deyà, P. M. Structure and Binding Energy of Anion- π and Cation- π Complexes: A Comparison of MP2, RI-MP2, DFT, and DF-DFT Methods. *J. Phys. Chem. A* **2005**, *109*, 4632–4637.
- (24) Runge, E.; Gross, E. K. U. Density-Functional Theory for Time-Dependent Systems. *Phys. Rev. Lett.* **1984**, *52*, 997–1000.
- (25) Zhu, X.; Thompson, K. C.; Martínez, T. J. Geodesic interpolation for reaction pathways. *J. Chem. Phys.* **2019**, *150*, 164103.

- (26) McInnes, L.; Healy, J.; Melville, J. UMAP: Uniform Manifold Approximation and Projection for dimension reduction. 2020; <https://arxiv.org/abs/1802.03426>.
- (27) Neese, F.; Wennmohs, F.; Becker, U.; Riplinger, C. The ORCA Quantum Chemistry Program Package. *J. Chem. Phys.* **2020**, *152*, 224108.
- (28) Huang, B.; von Lilienfeld, O. A. Quantum machine learning using atom-in-molecule-based fragments selected on the fly. *Nat. Chem.* **2020**, *12*, 945–951.
- (29) Christensen, A. S.; Faber, F. A.; Huang, B.; Bratholm, L. A.; Tkatchenko, A.; Müller, K.-R.; von Lilienfeld, O. A. qmlcode/qml: Release v0.3.1. 2017; <https://doi.org/10.5281/zenodo.817332>.